Soil Moisture Mapping Using ESTAR Under Dry Conditions From the Southern Great Plains Experiment (SGP99)

Aniruddha Guha, Jennifer M. Jacobs, Thomas J. Jackson, *Fellow, IEEE*, Michael H. Cosh, *Member, IEEE*, En-Ching Hsu, and Jasmeet Judge, *Member, IEEE*

***Abstract*—The electronically scanned thin array radiometer (ESTAR) was utilized for soil moisture mapping during the Southern Great Plains Experiment (SGP99). A retrieval algorithm was applied to obtain soil moisture from passive microwave measurements at 1.4 GHz. The algorithm was verified using ground data collected during SGP99. The results indicate a good correlation between observed and predicted soil moisture values and are consistent with results obtained from the same instrument in previous experiments. The present results demonstrate the validity of the retrieval algorithm for moderately to extremely dry soils. The ESTAR measurements along with ancillary data were used to create soil moisture maps of the entire region.**

***Index Terms*—Microwave, remote sensing, soil moisture.**

I. Introduction

THE FUNDAMENTAL principles of soil moisture retrieval using passive microwave sensors are well established [1]–[4] and have been used extensively in the last 25 years. Passive microwave soil moisture retrievals have been conducted using ground-based, airborne, and satellite sensors [5]–[9]. Field experiments—Walnut Gulch [10], Washita '92 [11], and SGP97 [12], in the Southern Great Plains and other regions of the United States—have collected passive microwave data as a part of an integrated set of hydrological data. In each of these experiments, the electronically scanned thin array radiometer (ESTAR) has provided L-band passive microwave measurements and provided reliable low error maps of surface soil moisture [10]–[12]. The ESTAR-derived soil moisture fields have been used extensively in studies of spatial soil moisture variability [13], [14], for assimilation in combination with land use and fractional vegetation cover to calculate regional heat fluxes [15], and to validate distributed land surface models in order to study the scaling behavior of modeled latent heat fluxes [16].

The Southern Great Plains Experiment 1999 (SGP99) provided an opportunity to relate L-band and C-band microwave measurements as several airborne and spaceborne sensors were used in conjunction with data collected on the ground. In addition to ESTAR, 4 different microwave instruments operating in the L- (1–2 GHz), S- (2–4 GHz), and C- (4–8 GHz) bands were flown on aircraft. The instruments included the Polarimetric Scanning Radiometer (PSR/C), the Step Frequency Microwave Radiometer (Step-C), and the Airborne C band Microwave Radiometer (ACMR) operating in the C-band and the Passive and Active L and S Band System (PALS) in the L- and S-bands. Passive microwave data were also collected by the Tropical Rainfall Measuring Mission (TRMM) satellite and the Special Sensor Microwave Imager (SSM/I) sensor.

This study provides continuity in the application of ESTAR measurements for soil moisture detection necessary to establish a long-term dataset of soil moisture, to evaluate the robustness of the soil moisture retrieval algorithm under a wide range of surface conditions, and to compare derived moisture products from other sensors. In this letter, we will validate the soil moisture retrieval algorithm under moderately to very dry conditions using ground data collected during SGP99 and ESTAR microwave brightness and provide regional soil moisture maps using the ESTAR soil moisture retrievals.

II. Study Region

This investigation is based on airborne and surface meteorological measurements from the Southern Great Plains region of the United States (Fig. 1). This region is characterized by a relatively homogeneous geography, variable surface flux properties, and large seasonal variation in temperature and specific humidity. The region is well instrumented for hydrological and atmospheric studies. The meteorological observation networks include the Department of Energy (DOE) Atmospheric Radiation Measurement Program (ARM) Cloud and Radiation Testbeds (CART), the United States Department of Agriculture (USDA) Agricultural Research Service (ARS) meteorological network within the Little Washita watershed, the Oklahoma Mesonet, and the USDA Natural Resources Conservation Service's (NRCS) two soil moisture and soil temperature (SMST) analysis network (SCAN) sites.

Intensive ground sampling was conducted in the Little Washita watershed near Chickasha, OK, El Reno, and the Central Facility during the experiment. The 603-km^2 Little Washita watershed lies in southwest Oklahoma. The topography is gently to moderately rolling with a 200-m maximum relief. The

Manuscript received January 27, 2003; revised July 1, 2003. This work was supported by the National Aeronautics and Space Administration under NASA NIP Grant NAG5-10567.

A. Guha, J. M. Jacobs, and E.-C. Hsu are with the Department of Civil and Coastal Engineering, University of Florida, Gainesville, FL 32611 USA.

T. J. Jackson and M. H. Cosh are with the Agricultural Research Service (ARS) Hydrology and Remote Sensing Laboratory, U.S. Department of Agriculture (USDA), Beltsville, MD 20705 USA.

J. Judge is with the Center for Remote Sensing, Agricultural and Biological Engineering Department, University of Florida, Gainesville, FL 32611 USA.

Digital Object Identifier 10.1109/TGRS.2003.817187

0196-2892/03$17.00 © 2003 IEEE

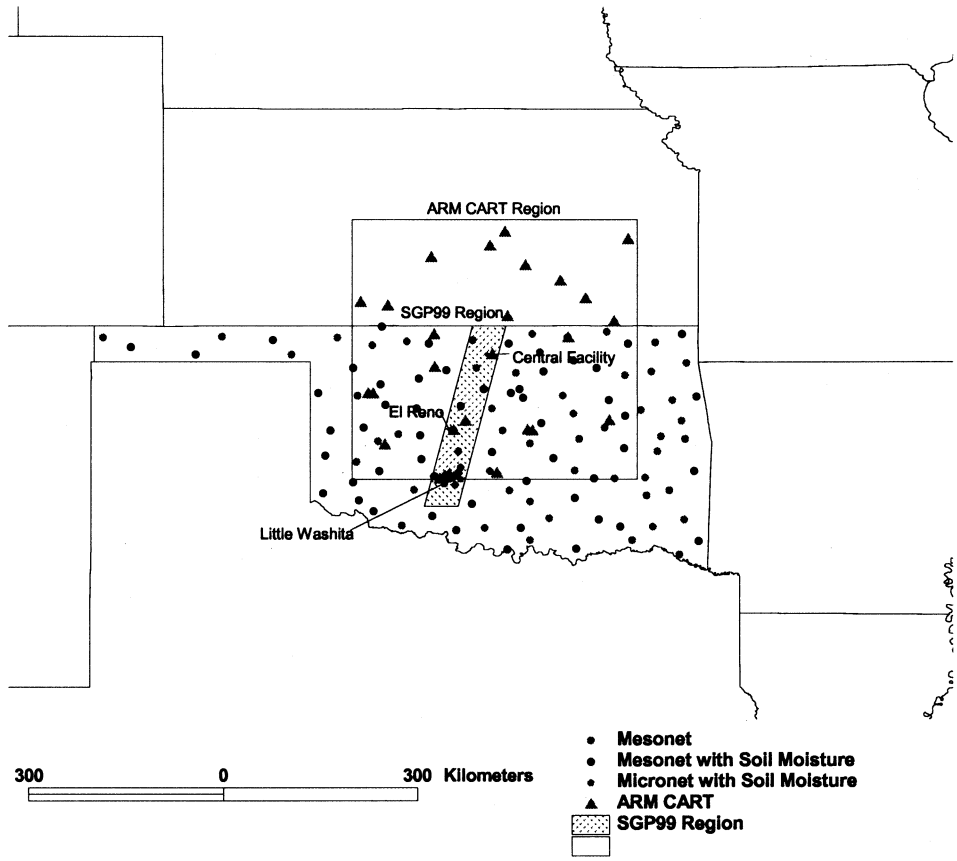

Fig. 1. SGP99 region with the various observation networks.

predominant land uses are rangeland and pasture with areas of winter wheat and other crops [17]. Soil texture is highly variable. The USDA ARS's 24.3-km^2 Grazinglands Research Laboratory in El Reno, OK has predominantly silty loam soils and winter wheat and natural prairie vegetation landcover. The DOE ARM Central Facility, located southeast of Lamont, OK, consists of pasture and winter wheat vegetation with silty loam soils.

III. Data and Methods

The soil moisture retrieval algorithm applied here uses ESTAR brightness temperatures along with surface temperature measured on the ground and land surface characteristics of roughness and vegetation. This retrieval algorithm is identical to that from previous ESTAR studies and is described by [4], [9]. The retrieval algorithm uses empirical relationships to determine the emissivity from a soil–water mixture and modifies the emissivity for the effects of soil roughness and vegetation.

A. ESTAR

ESTAR is a synthetic aperture microwave radiometer operating at a center frequency of 1.413 GHz (21 cm). ESTAR is a hybrid real and synthetic aperture radiometer. It obtains real aperture resolution along track and synthetic aperture resolution across track using a linear array of stick antennas. ESTAR measures horizontally polarized microwave data only. Details on ESTAR can be found in [11], [12], and [18], and data processing for SGP99 can be found in [19]. The data used here were those that had been resampled to a Lat Lon grid at a pixel resolution of 800 m after normalizing the viewing angle to nadir.

The ESTAR instrument was flown on a P-3B aircraft operated by NASA Wallops Flight Facility. Flights were conducted at an altitude of 7.6 km. As in the case of SGP97 the planned four parallel lines were modified to compensate for strong RFI in the vicinity of Oklahoma City. See [19] for more details on the flightlines. During the SGP99 period, six good days of data were collected by ESTAR-July 8, 9, 14, 15, 19, and 20.

B. Ground Sampling

Ground data collection was an integral part of SGP99 for soil moisture retrieval algorithm validation and also for checking the consistency of the sensors used during the experiment. The field sites were chosen using various criteria including relative location, proximity to instrumentation from one of the hydrological, and atmospheric observation networks and accessibility. Data were collected from 19 field sites in Little Washita, five in Central Facility, and six in El Reno. Each field was approximately 800 m $\times$ 800 m in size. Gravimetric soil moisture in each field was measured daily within a 3-h window to coincide with aircraft overflights. Two different field sampling protocols were utilized. In most fields, 14 samples were collected using a hand-held scoop and separated into two samples, one from the upper 1.0 cm and the other from 1.0–5.0 cm. Sampling was conducted along two transects separated by 400 m at 100-m intervals (full sampling). In the remaining fields, nine samples were collected over a 20 $\times$ 20 m grid (profile sampling). Coincident with the soil moisture measurements, soil temperatures

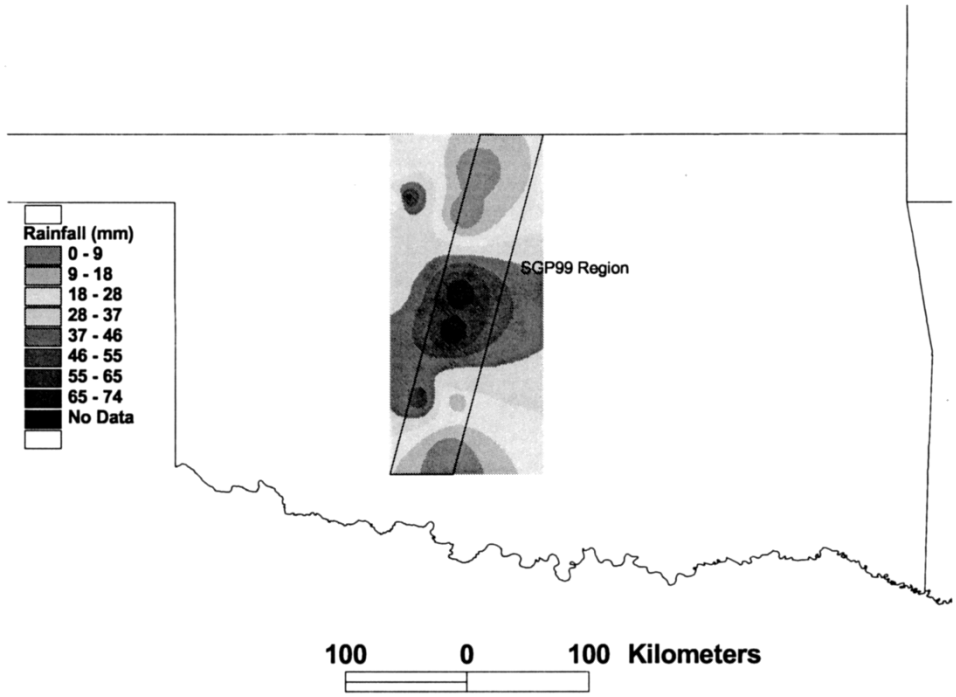

Fig. 2. Precipitation over the SGP region on July 10, 1999.

were measured at the surface and at several depths in the soil profile. The field bulk densities were measured separately. Bulk density measurements were used to determine the volumetric soil moisture from the gravimetric soil moisture content. The vegetation water content (VWC) and roughness were measured at least once in each field during the experiment.

C. Vegetation Characteristics

Vegetation effects for soil moisture retrieval are accounted for by a model proposed by Jackson and Schmugge [20] based on the relationship between optical depth and VWC. The relationship depends on the vegetation parameter (b) that is a function of the canopy type, polarization, and wavelength. The data used here were developed from a land cover classification performed using Landsat Thematic Mapper images by Jackson [21]. For each vegetation type, a vegetation parameter (b) was assigned based on published data. Vegetation water content was determined using NDVI values calculated using Landsat Thematic Mapper images of the region from July 15, 1999. The normalized difference vegetation index (NDVI) values were regridded and averaged to a spatial resolution of 800 m.

An empirically derived piecewise function was used as follows:

$$\mathrm{VWC} = 1.9134(\mathrm{NDVI})^2 - 0.3215(\mathrm{NDVI}), \qquad \mathrm{NDVI} \leq 0.5 \tag{1}$$

and

$$\mathrm{VWC} = 4.2857(\mathrm{NDVI})^2 - 1.5429, \qquad \mathrm{NDVI} > 0.5 \tag{2}$$

where VWC is measured in kilograms per square meter ($\mathrm{kg/m^2}$). For more details on the derivation of the VWC, see [12].

D. Surface Roughness and Soil Texture

Surface roughness results in the reflectivity of natural surfaces being somewhat higher than that of a smooth surface [4], [22]. Surface roughness was calculated based on [22]. For each land cover category, surface roughness was assigned based on previous investigations in this region. The algorithm utilizes an empirical mixing model [23] to calculate the effects of soil texture. Soil texture and porosity data were obtained from Pennsylvania State University's Earth System Science Center's (ESSC) CONUS-SOIL dataset [24].

E. Oklahoma Mesonet

The Oklahoma Mesonet is an automated environmental observing system distributed over the state of Oklahoma. There are 114 stations providing observations every 5 min. Each station consists of a 10-m tower providing measurements of air temperature (1.5 m), relative humidity (1.5 m), wind speed and direction (10 m), barometric pressure, rainfall, solar radiation, and soil temperature (10 cm for both sod and bare soil). The only significant rainfall event during the study period occurred on the evening of July 9 and the morning of July 10. The highest precipitation occurred in the ER region as seen in Fig. 2.

About half the stations provide supplemental measurements of air temperature (9 m), wind speed and direction (2 m), leaf wetness, soil moisture (5, 25, 60, and 75 cm under sod), and soil temperature (5 and 30 cm under sod and 5 cm under bare soil). The soil temperatures measured at the Mesonet stations were interpolated using an inverse distance weighting approach over the SGP region to create surface temperature maps. As Oklahoma Mesonet soil temperatures underestimated the surface temperatures measured in the fields during the experiment, the Mesonet soil temperatures were bias corrected to better reflect the measured surface temperatures during the retrievals.

TABLE I
VEGETATION AND SOIL PROPERTIES OF THE VARIOUS FIELD CLUSTERS USED IN SGP99

Field cluster	Sand %	Clay %	Bulk Density (g/cm^3)	VWC (kg/m^2)	Number of fields
LW	46.5	13.4	1.23	.479	19
CF	20.0	15.0	1.07	.261	5
ER	20.0	15.0	1.08	.646	6

IV. RESULTS OF THE SOIL MOISTURE ALGORITHM APPLICATION

The ESTAR data have a spatial resolution of 800 m. This scale is comparable to the average size of the validation field sites. As the georegistration of the sensor footprint is not more accurate than half the footprint size, the data from individual fields can not be used for validation studies. The fields were grouped together into three clusters of sites, Little Washita (LW), El Reno (ER), and Central Facility (CF) regions, and 518, 54, and 49 ESTAR pixels were averaged for LW, ER, and CF, respectively. Table I describes the soil parameters and the vegetation characteristics of these three sampling regions. Sensitivity studies have been carried out to determine the ability of the soil moisture retrieval algorithm to detect differences in soil moisture content [25]. It has been shown by [25] that the basic algorithm is capable of detecting differences in soil moisture when the VWC of the overlying vegetation is less than 3 kg/m^2. The conditions encountered in SGP99 were well within the range of the sensitivity of the soil moisture retrieval algorithm as can be seen from Table I.

A. Algorithm Validation

The extensive ground sampling of soil moisture conducted during SGP99 enables the evaluation of the retrieval algorithms. The soil moisture retrieval algorithm was validated by averaging the T_B, surface temperature, and all other parameters recorded over a cluster and using them to predict soil moistures. The observed T_B and soil moisture relationship is similar to the previously observed relationships for the same region [12]. Retrieved values were compared to the averages of the ground observed soil moistures from these sites. Fig. 3 shows the relationship between the predicted soil moisture and the *in situ* soil moisture measurements. The LW, CF, and ER predictions have R^2 values of 0.97, 0.96, and 0.94, respectively. The algorithm appears to have a small dry bias for this period. The ER region has the largest bias, particularly for the wetter conditions on July 14 and 15.

The results in [12] also underestimated measured soil moisture. This is likely a combination of the small sample size and the thatched grassland conditions. Among the five sampled fields in the ER region, significant variability was observed. The rms error between the predicted and observed values of volumetric soil moisture is 0.04. The rms error appears to decrease with decreasing soil moisture content. The higher soil moistures recorded from the ER region in Fig. 3 correspond to the localized event in the El Reno region. Although the sample size is limited in some regions and the ground conditions were quite dry in most cases, these results are comparable with other studies of soil moisture using ESTAR data.

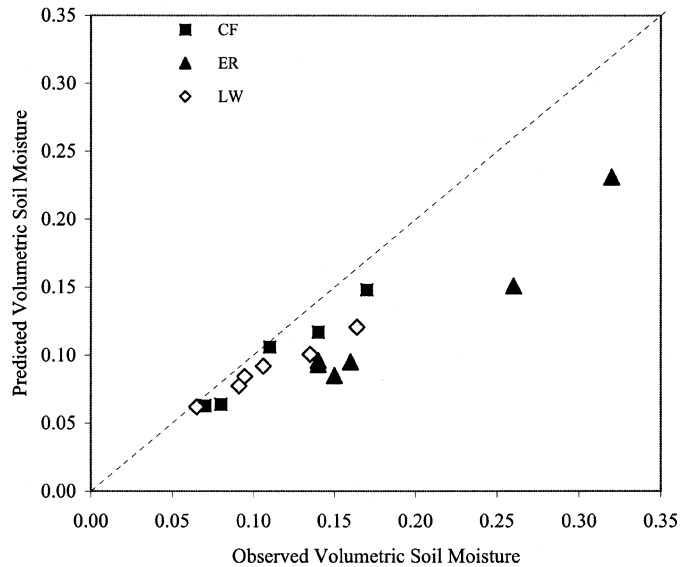

Fig. 3. Predicted versus observed values of volumetric soil moisture.

B. Soil Moisture Maps

The soil moisture algorithm was used for retrievals of soil moisture over the entire ESTAR footprint using the ancillary data described above. The results of the area retrievals can be seen in Fig. 4. The six days of ESTAR data include two brief drydown periods and one significant rain event on July 10. This rainfall event allows us to observe the redistribution of soil moisture in the region that results subsequent to a localized rainfall event. On July 14, three days after the rain, the wettest portion of the region is in the central and northern parts. While the greatest rainfall depth fell in the central region, portions of that region dried fairly quickly due to a a large area of relatively sandy soils [24]. In contrast, the northern region, having a more consistently high clay content, shows wetter soils. The July 15 image reflects the drydown. The precipitation signature is no longer evident in the July 19 and 20 images. The prerain event distribution on July 8 and 9 is very dry with low variability. The localized rain event, with its uneven distribution of rainfall, causes a high standard deviation of soil moisture on July 14. The rain event increases the mean from 0.12 to 0.16 and the standard deviation from 0.04 to 0.06. The strong drydown occurring from July 15 to 20 also greatly reduced the variability in soil moisture fields. Here, the measurement gaps limit observation during the drydown. Also, the time static nature of NDVI data does not allow us to model the effect of a change of VWC before and after the rain event. Regardless, the current research demonstrates the performance of the ESTAR instrument and soil moisture retrieval for the SGP99 experiment.

V. CONCLUSION

The methodology for soil moisture detection from mono-polarized microwave brightness temperatures was applied to L-band ESTAR data for the SGP99 experiment. The algorithm was verified using ground observations of soil moisture, surface

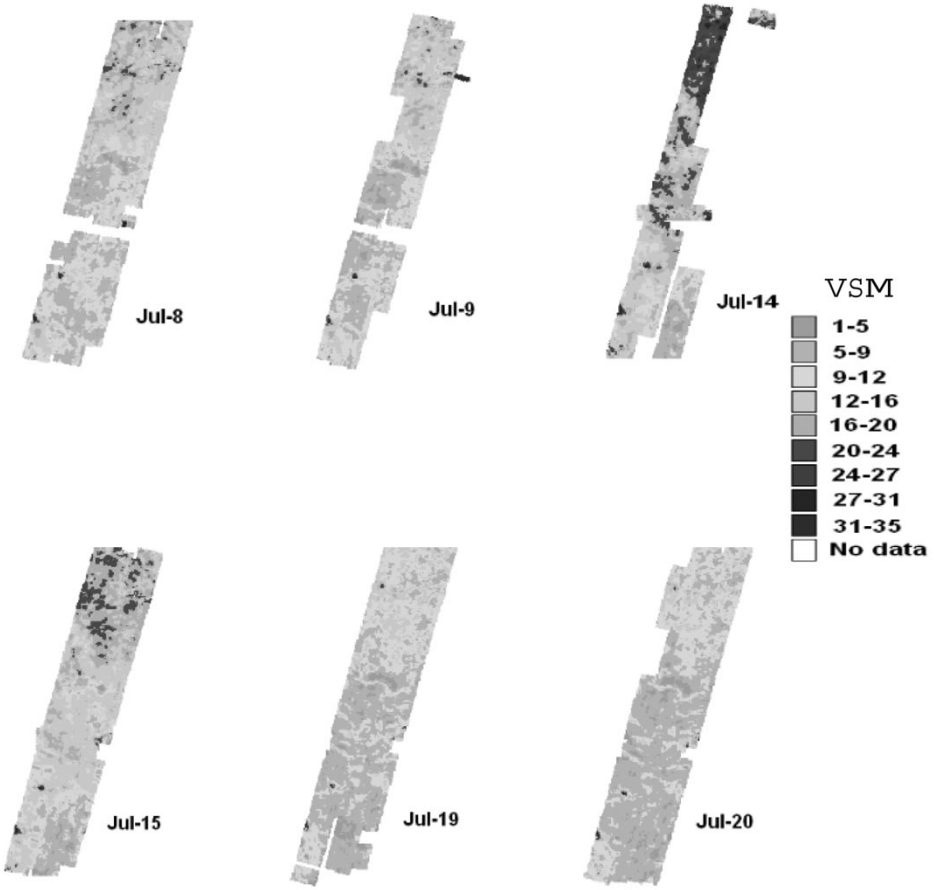

Fig. 4. Soil moisture maps of the SGP99 region.

temperature and vegetation biophysical characteristics. The results are comparable to previous studies using the same instrument. Climatic conditions during the field experiment did not allow the algorithms to be tested over a wide range of soil moisture conditions. However, the algorithm sucessfully characterized soil moisture, particularly for low soil moisture conditions. In addition, the presence of a rain event during the experiment provides observations of heterogeneous wetting and a brief drydown period. The research extends the ESTAR soil moisture dataset to include six days during the SGP99 experiment. The development of the SGP99 ESTAR soil moisture maps complements maps retrieved from PSR/C, TRRM, SSM/I, and PALS. This ESTAR dataset allows for comparisons of sensor performance and soil moisture results in addition to providing continuity to earlier microwave experiments.

ACKNOWLEDGMENT

The authors would like to acknowledge D. Le Vine's contributions to the processing of the ESTAR data. These data can be found at the NASA Distributed Data Archive site ftp://daac.gsfc.nasa.gov. The authors would also like to thank the efforts of four anonymous reviewers who helped make this letter significantly better. Oklahoma Mesonet data were provided as part of the NASA Terrestrial Hydrology and Aqua AMSR Programs.

REFERENCES

[1] F. T. Ulaby, R. K. Moore, and A. K. Fung, *Microwave Remote Sensing: Active and Passive*. Reading, MA: Addison-Wesley, 1981, vol. 1, Microwave Remote Sensing Fundamentals and Radiometry.

[2] ——, *Microwave Remote Sensing: Active and Passive*. Dedham, MA: Artech House, 1986, vol. 3, Volume Scattering and Emission Theory, Advanced Systems and Applications.

[3] T. J. Schmugge, "Techniques and applications of microwave radiometry," in *Remote Sensing in Geology*, B. S. Siegel and A. R. Gillespie, Eds. New York: Wiley, 1980.

[4] ——, "Remote sensing of soil moisture," in *Hydrological Forecasting*, M. G. Anderson and T. P. Burt, Eds. New York: Wiley, 1985.

[5] M. Owe, A. T. C. Chang, and R. E. Golus, "Estimating surface soil moisture from satellite microwave measurements and a satellite derived vegetation index," *Remote Sens. Environ.*, vol. 24, pp. 331–345, 1988.

[6] M. Owe, A. A. Van de Griend, and A. T. C. Chang, "Surface soil moisture and satellite passive microwave observations in semi-arid Southern Africa," *Water Resources Res.*, vol. 28, no. 3, pp. 829–839, 1992.

[7] E. G. Njoku and L. Li, "Retrieval of land surface parameters using passive microwave measurements at 6–18 GHz," *IEEE Trans. Geosci. Remote Sensing*, vol. 37, pp. 79–93, Jan. 1999.

[8] K. Y. Vinnikov, A. Robock, S. Qiu, J. K. Entin, M. Owe, B. J. Choudhury, S. E. Hollinger, and E. G. Njoku, "Satellite remote sensing of soil moisture in illinois, United States," *J. Geophys. Res.*, vol. 104, pp. 1103–1116, 2000.

[9] T. J. Jackson and D. M. Le Vine, "Mapping surface soil moisture using an aircraft-based passive microwave instrument: Algorithm and example," *J. Hydrol.*, vol. 184, pp. 85–99, 1996.

[10] T. J. Jackson, D. M. Le Vine, A. J. Griffis, D. C. Goodrich, T. J. Schmugge, C. T. Swift, and P. E. O'Neill, "Soil moisture and rainfall estimation over a semiarid environment with the ESTAR microwave radiometer," *IEEE Trans. Geosci. Remote Sensing*, vol. 31, pp. 836–841, July 1993.

[11] T. J. Jackson, D. M. Le Vine, C. T. Swift, T. J. Schmugge, and F. R. Schiebe, "Large area mapping of soil moisture using the ESTAR passive microwave radiometer in Washita-92," *Remote Sens. Environ.*, vol. 53, pp. 27–37, 1995.

[12] T. J. Jackson, D. M. Le Vine, A. Y. Hsu, A. Oldak, P. J. Starks, C. T. Swift, J. D. Isham, and M. Haken, "Soil moisture mapping at regional scales using microwave radiometry: The Southern Great Plains hydrology experiment," *IEEE Trans. Geosci. Remote Sensing*, vol. 37, pp. 2136–2151, Sept. 1999.

[13] Z. Hu, S. Islam, and Y. Cheng, "Statistical characterization of remotely sensed soil moisture images," *Remote Sens. Environ.*, vol. 61, pp. 310–318, 1997.

[14] A. Oldak, Y. Pachepsky, T. J. Jackson, and W. J. Rawls, "Statistical properties of soil moisture images revisited," *J. Hydrol.*, vol. 255, pp. 12–24, 2002.

[15] R. Bindlish, W. P. Kustas, A. N. French, G. R. Diak, and J. R. Mecikalski, "Influence of near-surface soil moisture on regional scale heat fluxes: Model results using microwave remote sensing data from SGP97," *IEEE Trans. Geosci. Remote Sensing*, vol. 39, pp. 1719–1728, Aug. 2001.

[16] C. D. Peters-Lidard, F. Pan, and E. F. Wood, "A re-examination of modeled and measured soil moisture spatial variability and its implications for land surface modeling," *Adv. Water Resources*, vol. 24, pp. 1069–1083, 2001.

[17] P. B. Allen and J. W. Naney, "Hydrology of the Little Washita River Watershed, Oklahoma: Data and analyses," U.S. Dept. Agriculture, Greenbelt, MD, ARS-90, vol. 74, 1991.

[18] D. M. Le Vine, A. Griffis, C. T. Swift, and T. J. Jackson, "ESTAR: A synthetic microwave radiometer for remote sensing applications," *Proc. IEEE*, vol. 82, pp. 1787–1801, 1994.

[19] D. M. Le Vine, T. J. Jackson, C. T. Swift, M. Haken, and S. Bidwell, "ESTAR measurements during the Southern Great Plains Eperiments (SGP99)," *IEEE Trans. Geosci. Remote Sensing*, vol. 39, pp. 1680–1685, Aug. 2001.

[20] T. J. Jackson and T. J. Schmugge, "Vegetation effects on the microwave emission of soils," *Remote Sens. Environ.*, vol. 36, pp. 203–212, 1991.

[21] T. J. Jackson, "Multiple resolution analysis of L-band brightness temperature for soil moisture," *IEEE Trans. Geosci. Remote Sensing*, vol. 39, pp. 151–164, Jan. 2001.

[22] B. J. Choudhury, T. J. Schmugge, A. T. C. Chang, and R. W. Newton, "Effect of surface roughness on the microwave emission from soils," *J. Geophys. Res.*, vol. 84, pp. 5699–5705, 1979.

[23] J. R. Wang and T. J. Schmugge, "An empirical model for the complex dielectric permittivity of soils as a function of water content," *IEEE Trans. Geosci. Remote Sensing*, vol. GE-18, pp. 288–295, 1980.

[24] D. A. Miller and R. A. White, "A conterminous united states multi-layer soil characteristics data set for regional climate and hydrology modeling," *Earth Interactions*, vol. 2, pp. 1–15, 1998.

[25] A. Guha and V. Lakshmi, "Sensitivity, spatial heterogeneity and scaling of C-band microwave brightness temperatures for land hydrology studies," *IEEE Trans. Geosci. Remote Sensing*, vol. 40, pp. 2626–2635, Dec. 2002.